

1 **Identifying and correcting the World War 2 warm anomaly**
2 **in sea surface temperature measurements**

3 **Comments are welcome by contacting the corresponding author directly.**

4 **Short title:** World War 2 sea surface temperature anomaly

5 Duo Chan ^{1*}, Peter Huybers¹

6 ¹Department of Earth and Planetary Sciences, Harvard University, USA

7 *Corresponding author. Email: duochan@g.harvard.edu

8 **Abstract**

9 Most foregoing estimates of historical sea surface temperature (SST) feature warmer global-
10 average SSTs during World War 2 well in excess of climate-model predictions. This warm
11 anomaly, referred to as the WW2WA, was hypothesized to arise from incomplete corrections of
12 biases associated with rapid changes in measurement instruments and protocols. Using linear
13 mixed-effects methods we confirm highly significant offsets among specific groups of bucket and
14 engine-room-intake SST measurements that, upon correction, reduce the WW2WA by 0.26°C
15 (95% c.i. 0.15 to 0.38°C). Furthermore, SST measurements during WW2 coming from buckets
16 are reportedly warmer at night than day, and controlling for this evident bias reduces the WW2WA
17 by another 0.05°C (0.02 to 0.08°C). Adjusted SSTs give a more stable and smoothly evolving
18 record of historical warming with a WW2WA of 0.09°C (-0.01 to 0.18°C) that is consistent with
19 internal variability in climate models.

20 INTRODUCTION

21 The two most recent versions of the extended-reconstructed SST (*1, 2*) both show an anomalous
22 warmth in global-mean SSTs that averages 0.28°C during 1941 to 1945 compared with the average
23 over the 10 surrounding years (1936 to 1940 and 1946 to 1950, Fig. 1 and Table 1). Version 4 of
24 the Hadley Center SST (HadSST4) shows a similar anomaly of 0.20°C (*3*). Such a warming
25 anomaly greatly exceeds that produced by any of the 94 historical CMIP5 simulations available
26 over this interval (*4*, gray shading in Fig. 1), as well as what can be explained by current knowledge
27 of climate forcing and internal variability using statistical models (*5*).

28 If the WW2 Warm Anomaly, WW2WA, reflects physical changes in climate, it would have
29 important implications for understanding the magnitude of decadal climate variability (*6-8*),
30 constraining uncertain external forcing (*9*), and partitioning relative contributions of
31 anthropogenic forcing and internal variability in driving historical climate change (*10-13*). For
32 example, such an anomaly could indicate the ability of the El Niño Southern Oscillation (ENSO)
33 to lead to larger and more persistent warming than is typically observed (*14*).

34 However, the physicality of the WW2WA is questionable. Different instrumental
35 estimates disagree on the SST evolution during WW2 (Fig. 1). Despite highly significant warm
36 spikes in ERSSTs and HadSST4, HadSST2 (*15*) was shown to exhibit a step in global-average
37 SST of 0.3°C once the effects of variations in Niño and ocean-land atmospheric effects were
38 filtered from the global average (*16*), and the WW2WA was essentially absent in HadSST3 (*17*).
39 Furthermore, neither air temperatures from near-shore weather stations (*18*) nor temperature
40 proxies derived from isotopes in Tropical coral reefs (*19*) show a similar WW2 anomaly.

41 **Hypothesized causes and existing corrections**

42 The presence of discontinuities in the SST record appears especially likely an artifact because of
43 a major transition in instruments (16) changes in protocols (20), and a 58% reduction in the number
44 of SST measurements during the WW2 interval (17). It has been suggested that the WW2WA
45 occurs because the dominant data-collecting instrument alternates from buckets in the five years
46 prior and post WW2 to engine-room-intake (ERI) during 1941 to 1945 (16). Bucket SSTs are
47 generally biased cold from evaporative and sensible cooling, with the cold bias of a typical U.K.
48 canvas bucket estimated to average 0.4°C (21). Conversely, although ERI measurements are
49 typically extracted from 5 to 15m below the surface and are consequently cooler than true SSTs
50 defined at depths of 20 to 30 cm (3). ERI SSTs have an average warm bias of 0.1 to 0.3°C because
51 of absorption of heat from ship engines (3, 17).

52 A second hypothesis involves changes in protocols for taking measurements at night.
53 Night-time marine air temperature reading is known to have been taken in-board in order to avoid
54 detection and, consequently, to be warmly biased by approximately 0.8°C (20). We speculate that
55 bucket SSTs were also read in-board during WW2. The fact that the proportion of SST readings
56 during day shifts from 55% of the total in the surrounding ten years of the war to 61% between
57 1941 and 1945 also suggests a preference for avoiding night-time readings. Incomplete corrections
58 of biases among ERI and bucket measurements could be responsible for the WW2WA.

59 The six major SST estimates covering the WW2 period each account for SST biases using
60 distinct methods. Because these estimates all rely upon data coming from the International
61 Comprehensive Ocean-Atmosphere Data Set (ICOADS, 22), differences among estimates
62 generally arise from differences in correction schemes that can be divided into two groups. In one

63 approach, bucket and ERI measurements are not distinguished and average SSTs are corrected to
64 follow independent estimates of temperatures. For example, ERSST5 (2) is referred to Hadley
65 night-time marine air temperatures (23), from which the global average inherits a 0.22°C warm
66 anomaly during WW2 relative to the ten surrounding years. Note that our taking the average
67 between 1941 and 1945 relative to the average over the prior and subsequent five years accounts
68 for the potential of an underlying linear trend between 1936 and 1950. Ship-based air temperatures
69 are, however, potentially subject to their own biases on account of non-standard measurement
70 practices (20) and reconstruction choices (23) during WW2. Another example is to reference SSTs
71 to air temperature from coastal and island weather stations, in which case the WW2 SST anomaly
72 is removed (18).

73 A second approach to correcting SSTs distinguishes between bucket and ERI
74 measurements and attempts to correct their respective biases (3, 17). A major impediment to such
75 corrections, however, is that measurement methods are poorly documented during WW2, with
76 only 6% of observations being specifically documented as coming from buckets, 11% from ERIs,
77 and 83% undetermined (22, 24). The magnitudes of SST biases are also uncertain, and, as noted,
78 may have changed during WW2 (20, 23). The lack of information regarding measurements has
79 been addressed through plausible but uncertain assumptions. In constructing HadSST3, for
80 example, it was assumed that U.S. and U.K. naval ships with unknown methods make ERI
81 measurements of SST that are, on average, warmly biased by 0.2°C (17). HadSST4, however,
82 randomly designates unknown measurements during WW2 to be either bucket or ERI SSTs, with
83 the portion of bucket measurements ranging from 0 to 25%. Wartime ERI measurements in
84 HadSST4 are specified to have a 0.25°C warm bias, on average, whereas buckets are specified to
85 have a -0.2°C cold bias (3).

86 **RESULTS**

87 **Groupwise SST offsets**

88 We examine hypotheses that changes in instrumental and measurement protocols account for the
89 WW2WA using a linear-mixed-effects (LME) methodology. This LME method was recently
90 shown to accurately identify offsets among groups of bucket SST measurements in the ICOADS
91 dataset (25,26), and we extend the approach to encompass ERI measurements (Fig. S1). SST
92 measurements coming from distinct groups that are within 300 km and 2 days of one another are
93 differenced (Fig. 2D), and systematic structures in the differences are partitioned among regional,
94 seasonal, temporal, and groupwise offsets. Groups are defined according to instrument type,
95 nation, and 'decks', where the term 'deck' originally refers to punch cards that marine observations
96 were encoded upon (22). Although decks were not necessarily originally organized according to
97 physical features, in practice, there are major offsets between different decks of bucket
98 measurements (25). Variance not attributable to systematic offsets by our LME method is
99 considered noise that is parameterized in relation to location, season, and distance in space and
100 time between measurements (see methods). Importantly, the LME methodology permits for
101 obtaining groupwise offsets regardless of whether the method of measurement is known.

102 Of the 66 groups present between 1935 and 1949, 29 have significant offsets ($P < 0.05$,
103 Table S1). Significance is assessed relative to a null hypothesis of zero-mean offset with respect
104 to the average across all groups. After correcting for multiple hypothesis testing using a
105 Bonferroni correction, 12 groups still show significant offsets ($P < 0.05/n$, $n=66$). There are five
106 positively identified ERI groups that are found to be warmer than the 24 bucket groups, on average,
107 by 0.53°C (0.25 to 0.72°C , Table S1). All uncertainties are reported as 95% coverage intervals
108 unless otherwise noted. Offsets of unknown groups range from -0.4 to 0.6°C , a range similar to

109 that spanned by the entire population of the bucket and ERI groups, suggesting that at least some
110 of these groups are distinctly from bucket or ERI measurements.

111 A check of our estimated groupwise offsets is afforded through comparing against the
112 amplitude of the diurnal cycle associated with individual groups. ERI measurements typically
113 come from greater depths and, thus, exhibit a smaller amplitude diurnal cycle than actual SSTs,
114 whereas buckets are subject to solar gain and generally exhibit a larger amplitude diurnal cycle
115 (27). A strong correlation emerges between diurnal amplitudes and offsets among groups
116 consistent with many groups containing a mixture of bucket and ERI measurements (28).
117 Extending the same techniques to measurements of unknown origin (Fig. 3), we find that most
118 U.S. measurements that are biased warm also exhibit a small diurnal amplitude, consistent with
119 their being ERI measurements. Specifically, five U.S. groups (deck 110, 116, 195, 281, and 705)
120 account for 88% of all U.S. measurements during 1935 to 1949 and each is significantly warmer
121 than the average across all groups ($P < 0.05$, Fig. 3, Table S1) and exhibits a diurnal amplitude that
122 is significantly smaller ($P < 0.05$, Fig. 3, Table S1, and Fig. S2) than a climatology derived from
123 drifting buoys (see methods). The combination of warm offsets and small diurnal amplitudes
124 confirm the assumption in HadSST3 that U.S. measurements with missing method information
125 during WW2 are ERI measurements.

126 Although it is not necessary to identify the instrumental origin of measurements in order
127 for our method to estimate and correct for offsets, we first make a provisional classification of
128 measurements with unknown instrumental information for purposes of estimating SSTs using
129 bucket-only and ERI-only measurements. In particular, we assign all U.S. ships of unknown origin
130 to ERIs because of their anomalously warm offsets and anomalously small diurnal amplitudes
131 (Table S1). Estimates of global-average SSTs using only observations thought to come from ERIs,

132 0.09°C, or buckets, 0.19°C, are stable through WW2 relative to the warming shown in the raw
133 ICOADS data, 0.41°C (Fig. 2A), confirming that the anomaly mainly reflects instrumental changes
134 at the start and the end of the war (16).

135 Our main line of reconstruction of historical SSTs during WW2 relies on combining all
136 groups of SSTs together after correcting for groupwise offsets, which gives an estimate of global
137 SSTs featuring a WW2WA that is decreased from 0.41°C in the raw ICOADS measurements (Fig.
138 2A) to 0.14°C (0.02 to 0.27°C) in the groupwise corrected SSTs (Fig. 2B). Groupwise adjusted
139 SSTs are consistent between bucket and ERI-only estimates, with collocated ERI minus bucket
140 difference decreasing from an average of 0.48°C over 1936 to 1950 in raw ICOADS3.0 to being
141 centered on zero after adjustments (Fig. 2C).

142 Diminishment of the WW2WA reflects negative adjustments of SSTs from U.S. Navy ship
143 logs (deck 195) that have a warm offset of 0.43°C (0.17 to 0.68°C) that alone brings the WW2WA
144 from 0.41°C in raw ICOADS to 0.22°C (Fig. 2E). Also of note are U.K. Royal Navy ship logs
145 (deck 245) that have a data gap in 1940 (Fig. S1A) and offsets that are -0.31°C (-0.53 to -0.09°C)
146 cold before 1940 and 0.25°C (0.03 to 0.47°C) warm over 1941-1947 (Fig. 3). Adjusting offsets in
147 deck 245 contributes another 0.06°C to the diminishment of the WW2WA (Fig. 2E), with the
148 largest local decrease of more than 0.4°C over the Indian Ocean and the Pacific Warm Pool.

149 **Night-time bucket SSTs**

150 The second hypothesis we test is whether warm biases arise as a result of measuring bucket SSTs
151 in-board during the night. When isolated, raw night-time bucket measurements contain a 0.32°C
152 warm anomaly during the war (Fig. 4A). Night-time SSTs reverse from being cooler than
153 collocated daytime temperatures by -0.20°C during the five years before and after WW2, as

154 expected regardless of bucket design (28) to actually being 0.02°C warmer during WW2.
155 Spatially, warm WW2 night-time bucket SSTs are found over the Indian Ocean and the extra-
156 tropical Atlantic (Fig. 4B). No such night-time-warming anomaly is found in measurements
157 coming from ERIs. Furthermore, the WW2WA is consistent between raw daytime bucket SSTs
158 (0.10°C, Fig. 4A) and raw daily-mean ERIs (0.09°C, Fig. 2A and 4C).

159 The inversion of the diurnal cycle in bucket SSTs during WW2 is mainly attributable to
160 British Navy ships (deck 204) that contribute more than 75% of open-ocean bucket SSTs during
161 1942 to 1945. (SST observations from buckets that are concentrated near shore have little overall
162 influence on global SST estimates after gridding.) When resolved at the hourly resolution, SST
163 anomalies from deck 204 show a diurnal cycle that peaks at 4 pm and has a diurnal amplitude that
164 is 0.04°C higher than drifters in the ten years surrounding WW2. During WW2 the diurnal peak
165 of deck 204 occurs at 8 pm, and the amplitude of the diurnal cycle is 0.03°C smaller than drifters
166 (Fig. S3). The smaller diurnal amplitude is unlikely to relate to switching to ERI measurements
167 in decks 204 because the average temperature of daytime measurements remains both consistent
168 with bucket measurements and cooler than known ERI measurements taken before and after WW2.
169 These results are consistent with both night-time marine air temperatures (20) and bucket
170 temperatures being measured in-board during WW2. British Naval group deck 245 exhibits a
171 similar, albeit less dramatic, decrease in the amplitude of the diurnal cycles (Fig. 3).

172 Although our LME method could be further extended to temporally resolve anomalies in
173 night-time biases, building in such flexibility would essentially make night-time temperatures
174 uninformative. Instead, we simply repeat our analysis using only daytime measurements.
175 Specifically, we use 24.1 million pairings of SST measurements between 1850 and 2014 with 1.1
176 million of these pairs available between 1935 and 1950. Whereas using both day and night

177 measurements gives a 0.14°C (0.02 to 0.27°C) WW2WA, the daytime-only analysis gives a
178 WW2WA of 0.09°C (-0.01 to 0.18°C , Table 1, Fig. S4). Sampling hourly-resolved climatological
179 diurnal cycles from drifters indicates that the shift from 55% of observations occurring in the
180 daytime in the five years before and after WW2 to 61% during WW2 accounts for only 0.005°C
181 of the anomaly, with the systematically warmer night-time temperatures inferred to account for
182 the majority of the difference.

183 The CMIP5 ensemble of 25,236 years of pre-industrial simulations indicates a 0.10°C
184 anomaly in global SSTs as the 95% value for all 15-year intervals (see methods). The residual
185 warm anomaly found after groupwise correction to daytime-only data, therefore, accords with
186 internal SST variability (Fig. 5B). Also consistent with internal variability are bucket-only
187 estimates of SST, having a WW2WA of 0.08°C (-0.02 to 0.17°C) and ERI-only estimates having
188 an anomaly of 0.04°C (-0.07 to 0.14°C). This revision from SST anomalies being highly
189 inconsistent between observations and simulations during WW2 to being consistent, after
190 accounting for observational biases, may also point to a means of resolving the greater SST
191 variance in observational data relative to simulations found at decadal and longer timescales (29).

192 **DISCUSSION**

193 **Comparison with other estimates**

194 The SST adjustments obtained through our LME approach agree with an independent estimate
195 arrived at using near-shore, land-station data (18, Fig. 5A). Whereas the approach of ref. (18)
196 requires average SSTs to agree with land-station data, our analysis shows that the WW2 warm
197 anomaly is an artifact arising from specific groups and features of SST measurements. Our results

198 confirm the assumption made in ref. (18) that trends derived from land-station data are more
199 dependable during WW2 than those coming from uncorrected SSTs.

200 Compared with corrections in HadSST, our groupwise intercomparison suggests that ERI
201 and bucket groups have an average offset of 0.53°C (0.25 to 0.72°C), nearly 0.1°C greater than the
202 0.45°C difference used in HadSST4. Furthermore, our analysis indicates that unknown U.S. and
203 U.K. measurements during 1942 to 1945, which account for 98% of unknown wartime
204 measurements, are offset warm. In HadSST4, 12.5% of the unknown measurements were assumed
205 to be offset cold and corrected as if from buckets. The smaller offset assumed between bucket and
206 ERI SSTs and a higher percentage of observations assumed to come from buckets explains the re-
207 emergence of the WW2WA in HadSST4. Finally, whereas HadSST4 assumes large uncertainties
208 in data origin during WW2, our analysis uses relative offsets to provide corrections and reduces
209 the standard error of WW2WA from 0.14°C in HadSST4 to 0.05°C in our estimates.

210 An important attribute of groupwise adjustments is the ability to resolve regional biases
211 arising from spatially heterogeneous distributions of distinct groups (Fig. S5). Removing
212 groupwise offsets leads to a greater decrease in the WW2WA over the Indian ocean and Pacific
213 Warm Pool and smaller decreases over the Tropical Eastern Pacific and the South Atlantic (Fig.
214 S5B). The spatial correlation of WW2 anomalies between our adjustments and adjusted daytime-
215 only estimates is $r_s = 0.02$, where r_s indicates the Pearson cross-correlation taken across space and
216 its small value indicates that the magnitude of the pattern that we remove is appropriate. HadSSTs
217 partially accounts for biases associated with shifting instruments and has a similar pattern of
218 correction albeit one that is smaller such that $r_s = -0.15$ (Fig. S5E) for HadSST3 and -0.18 for
219 HadSST4 (Fig. S5F). In contrast, ERSST products use a fixed spatial pattern (1,2) that is unable
220 to correct for local patterns of spatial bias giving a $r_s = -0.30$ for ERSST4 (Fig. S5D) and $r_s = -$

221 0.31 for ERSST5. The zonally symmetric corrections from ref. (18) are also ineffective at
222 removing the WW2 pattern of offsets.

223 In addition to the removal of the WW2WA, our adjustments give a more stable and smoothly
224 evolving SST estimate (table 1). The 1936 to 1950 variance of global-average, annual SST
225 anomalies decreases from $5.6 \times 10^{-2} \text{C}^2$ in ICOADS raw to $0.5 \times 10^{-2} \text{C}^2$ in the adjusted daytime-
226 only estimates. Such sub-decadal variability is consistent with estimates from HadSST3 and
227 Cowtan SST and lies within the 95% confidence interval of CMIP5 simulations. In contrast,
228 HadSST4 and ERSSTs have significantly higher variance estimates ($P < 0.05$). On regional scales,
229 the effect of groupwise adjustments is smaller compared with physical variability, sampling
230 uncertainty, and random measurement errors, such that the 1936 to 1950 variance on $5^\circ \times 5^\circ$ grids
231 decreases by approximately 20%, on average.

232 **Conclusion**

233 The WW2WA in instrumental SST estimates has long been suggested to be a data artifact that
234 arises from instrumental changes (16). Our analysis confirms the existing hypothesis, identifies
235 warm biases in WW2 night-time SSTs, and provides corrections that remove the WW2WA at both
236 global and regional scales. This adjustment leads to a more homogeneous trend in SSTs and
237 reconciles the largest discrepancy between historical surface temperatures and models (5),
238 bringing SST estimates into accord with estimates of forcing, climate sensitivity, and internal
239 variability. Our results also highlight the importance of further resolving heterogeneity in
240 historical SSTs (24, 26, 30, 31). Adjusting measurements at the level of individual ships (32, 33)
241 in future work may permit more detailed corrections and may reveal even more homogeneous
242 trends in SST.

243 **Materials and Methods**

244 **Grouping**

245 After the same quality control procedures as in ref. (25), sea surface temperatures (SSTs) from
246 ICOADS 3.0 (22) are grouped according to nation, deck, and measurement method. Nation is
247 identified first using ICOADS country code (C1, 22). When C1 is not available, nation is inferred
248 from ship call signs (26, 28) or deck information (17, 25). If still unidentified, nations information
249 is considered missing, and associated SSTs are grouped only according to deck and method
250 information. Deck is the primary metadata for tracking ICOADS data collections and is available
251 for all SST measurements in ICOADS. Decks having the same description in ICOADS and are
252 combined as in ref. (28). Measurement method is identified from ICOADS SST measurement
253 method (SI) metadata. When SI is not available, we use information from the World Meteorology
254 Organization No. 47 publication (WMO No.47). If both are not available, we assign measurement
255 method to be unknown. There are cases that SI and WMO No.47 do not agree (27), this, however,
256 does not affect results during WW2 because WMO No.47 becomes available in ICOADS after the
257 1960s.

258 **Groupwise adjustment**

259 Groupwise adjustments to SSTs are estimated using a linear-mixed-effects (LME) model,

$$260 \quad \delta\mathbf{T} = \mathbf{X}\boldsymbol{\alpha} + \mathbf{Z}_y\boldsymbol{\beta}_y + \mathbf{Z}_r\boldsymbol{\beta}_r + \boldsymbol{\beta}_\sigma \quad (1)$$

261 The vector of temperature differences, $\delta\mathbf{T}$, is determined from pairs of SST observations that are
262 associated with different nation-deck-method group assignments and are within 300 km and 2 days
263 of one another. All SST measurements that are identified to come from bucket, ERI, hull sensor,

264 or unknown methods between 1850 and 2014 are analyzed for purposes of fully accounting for
265 information outside WW2 of focus. We identify a total of 45.8 million pairs of SSTs, which
266 comprises a subset of 1.8 million SST differences during 1935 to 1950.

267 SST differences contained in $\delta\mathbf{T}$ are represented as a 'fixed-effect' term describing offsets
268 between groups, α , and random effects describing temporal variations (five-year blocks), β_y , and
269 regional variations (17 sub-basin regions), β_r . Matrices \mathbf{X} , \mathbf{Z}_y , and \mathbf{Z}_r specify, respectively,
270 common pairs of nations, five-year blocks, and sub-basins. β_σ is the residual. Offsets are estimated
271 relative to the mean of all paired measurements.

272 More details on the LME design and implementation is available in a methodology paper
273 (25). In an update to ref. (25), the analysis presented here intercompares both bucket and engine-
274 room-intake SSTs and, therefore, yields a total of 492 groups each contributing to at least 5,000
275 pairs of SST observations. In addition, to account for seasonal variations in groupwise offsets,
276 LME models are run for subsets of consecutive three months and repeated twelve times with the
277 central month sliding from January to December. Months of Southern Hemisphere SSTs are
278 shifted by half of a year to account for different seasons between hemispheres.

279 Uncertainties of groupwise offsets, ϵ_g , are quantified by the LME methodology and
280 associated 95% c.i. of individual offsets are estimated as marginal distributions assuming that
281 offsets follow a multivariate normal distribution (25). As noted in previous studies (26, 34),
282 random errors (ϵ_r) that arise from partial sampling and observational noise become negligible under
283 global and decadal averaging, whereas ϵ_g is partially systematic. We, therefore, only quantify and
284 report uncertainties that stem from ϵ_g for adjusted SSTs. Uncertainties in groupwise adjustments

285 are realized by a 1000-member ensemble of random adjustments that perturb groupwise offsets
286 using their error estimates in keeping with covariance and spatial structures (26).

287 The LME method estimates groupwise offsets relative to the mean of all paired
288 measurements and does not account for common biases shared by all groups. Biases between
289 bucket and engine-room-intake measurements may vary with time. One example is that night-
290 time SSTs are abnormally warm from 1941 to 1945 (Fig. 4A), which increases common biases
291 during WW2 and results in a residual warm anomaly after adjusting for groupwise offsets. To
292 exclude the influence of WW2 biases in night-time SSTs, we perform another LME analysis with
293 the same model setup but using only daytime measurements. The daytime-only analysis makes
294 use of a total of 24.1 million SST pairs throughout 1850 to 2014, with a subset of 1.1 million pairs
295 between 1935 and 1950. Another example of changing common biases involves systematic
296 changes from less-insulated canvas to more-insulated rubber buckets (17). However, the overall
297 change in bucket types have been estimated to happen after the 1950s (17) or gradually take place
298 from the 1930s to the 1970s (3). In either case, the associated changes in common biases will have
299 a small influence on the WW2WA.

300 **Diurnal Cycle**

301 Recent studies (27, 28) illustrate the utility of using the diurnal cycle for better understanding
302 biases in historical SST measurements. In this study, diurnal cycles of individual groups are
303 calculated using tracked ships (35) following the methodology of ref. (28). Only 33 out of 66 ship
304 groups have acceptable estimates of diurnal cycles, whereas the others have issues arising from
305 lack of tracked ships or insufficient measurements distributed across the day. Diurnal amplitudes
306 are estimated using data between 1935 and 1949 using a least-squares fit of a once-per-day sinusoid

307 (28). The diurnal amplitude of U.S. deck 195 is determined by a least-squares fit using the diurnal
308 cycles determined from bucket- and ERI-only measurement, where this special approach is taken
309 because of the large number of measurements U.S. deck 195 contributes but its having an
310 insufficient sampling frequency to independently constrain its amplitude (see Fig. S2 for more
311 details). To account for distinct spatial and seasonal coverage of individual groups, reported
312 diurnal amplitudes in Fig. 3 are anomalies relative to 1990 to 2014 climatological amplitudes
313 estimated from drifting buoys (25). The scaling between diurnal amplitudes and groupwise offsets
314 is estimated using a York regression (36) and associated uncertainties are estimated by
315 bootstrapping individual groups 10,000 times with replacement.

316 **Comparison with other estimates**

317 There are different versions of the ICOADS dataset that have been used in various studies, but
318 these differences should have limited influence on SST biases during WW2. First, whereas
319 Cowtan SST (18), HadSST3 (17), and ERSST4 (1) are based on ICOADS2.5 (37), our adjusted
320 SSTs, HadSST4 (3), and ERSST5 (2) are based on ICOADS3.0 (22). Compared with 7.4 million
321 measurements over 1935 to 1949 in ICOADS2.5, ICOADS3.0 only includes an additional 17
322 thousand measurements from the U.S. lightship collection. Second, we make use of only ship-
323 based measurements, but other datasets also make use of measurements from moored and drifting
324 buoys and the coastal-marine automated network, but which only become available after the 1980s.
325 Third, ERSSTs and Cowtan SST infill monthly grid boxes without data, but our estimates and
326 HadSSTs leave these boxes unfilled. Finally, ERSSTs and Cowtan SSTs provides only central
327 estimates, whereas our adjusted SSTs and HadSSTs provide publicly available ensembles that
328 allow for estimating uncertainties associated with corrections.

329 To compare in-situ SST estimates with model simulations, we make use of 94 historical
330 runs from 39 CMIP5 models and a total of 25,236 years of pre-industrial simulations (4) that we
331 re-grid to a common 5° resolution. Pre-industrial runs are segmented into consecutive 15-year
332 segments. We then mask each historical run using the monthly coverage in ICOADS3.0 and each
333 15-year pre-industrial segment using the ICOADS coverage between 1936 and 1950. The mean
334 difference between the central five years (1941 to 1945) and surrounding ten years (1936 to 1940
335 and 1946 to 1950) is then calculated for individual pre-industrial segments (historical runs).

336

337 **References**

- 338 1. Huang, B. et al. Extended reconstructed sea surface temperature version 4 (ERSST. v4).
339 Part I: Upgrades and intercomparisons. *Journal of Climate* 28, 911–930 (2015).
- 340 2. Huang, B. et al. Extended reconstructed sea surface temperature, version 5 (ERSSTv5):
341 upgrades, validations, and intercomparisons. *Journal of Climate* 30, 8179–8205 (2017).
- 342 3. Kennedy, J., Rayner, N., Atkinson, C. & Killick, R. An ensemble data set of sea surface
343 temperature change from 1850: The Met Office Hadley Centre HadSST. 4.0.0.0 data set.
344 *Journal of Geophysical Research: Atmospheres* 124, 7719–7763 (2019).
- 345 4. Taylor, K. E., Stouffer, R. J. & Meehl, G. A. An overview of CMIP5 and the experiment
346 design. *Bulletin of the American Meteorological Society* 93, 485–498 (2012).

- 347 5. Folland, C. K., Boucher, O., Colman, A. & Parker, D. E. Causes of irregularities in trends
348 of global mean surface temperature since the late 19th century. *Science Advances* 4,
349 EAAO5297 (2018).
- 350 6. Hansen, J., Ruedy, R., Sato, M. & Lo, K. Global surface temperature change. *Reviews of*
351 *Geophysics* 48 (2010).
- 352 7. Morice, C. P., Kennedy, J. J., Rayner, N. A. & Jones, P. D. Quantifying uncertainties in
353 global and regional temperature change using an ensemble of observational estimates: The
354 HadCRUT4 data set. *Journal of Geophysical Research: Atmospheres* 117 (2012).
- 355 8. Vose, R. S. et al. NOAA's merged land–ocean surface temperature analysis. *Bulletin of*
356 *the American Meteorological Society* 93, 1677–1685 (2012).
- 357 9. Stevens, B. Rethinking the lower bound on aerosol radiative forcing. *Journal of Climate*
358 28, 4794–4819 (2015).
- 359 10. Jones, G. S., Stott, P. A. & Christidis, N. Attribution of observed historical near–surface
360 temperature variations to anthropogenic and natural causes using CMIP5 simulations. *Jour-*
361 *nal of Geophysical Research: Atmospheres* 118, 4001–4024 (2013).
- 362 11. Bindoff, N. L. et al. Detection and attribution of climate change: from global to regional
363 (2013).
- 364 12. Maher, N., Gupta, A. S. & England, M. H. Drivers of decadal hiatus periods in the 20th
365 and 21st centuries. *Geophysical Research Letters* 41, 5978–5986 (2014).

- 366 13. Hegerl, G. C., Brönnimann, S., Schurer, A. & Cowan, T. The early 20th century warming:
367 anomalies, causes, and consequences. *Wiley Interdisciplinary Reviews: Climate Change* 9,
368 e522 (2018).
- 369 14. Thompson, D. W., Wallace, J. M., Jones, P. D. & Kennedy, J. J. Identifying signatures of
370 natural climate variability in time series of global-mean surface temperature: Methodology
371 and insights. *Journal of Climate* 22, 6120–6141 (2009).
- 372 15. Rayner, N. et al. Improved analyses of changes and uncertainties in sea surface tempera-
373 ture measured in situ since the mid-nineteenth century: the HadSST2 dataset. *Journal of*
374 *Climate* 19, 446–469 (2006).
- 375 16. Thompson, D. W., Kennedy, J. J., Wallace, J. M. & Jones, P. D. A large discontinuity in
376 the mid-twentieth century in observed global-mean surface temperature. *Nature* 453, 646–
377 649 (2008).
- 378 17. Kennedy, J., Rayner, N., Smith, R., Parker, D. & Saunby, M. Reassessing biases and other
379 uncertainties in sea surface temperature observations measured in situ since 1850: 2. biases
380 and homogenization. *Journal of Geophysical Research: Atmospheres* 116 (2011).
- 381 18. Cowtan, K., Rohde, R. & Hausfather, Z. Evaluating biases in sea surface temperature
382 records using coastal weather stations. *Quarterly Journal of the Royal Meteorological*
383 *Society* 144, 670–681 (2018).
- 384 19. Pfeiffer, M. et al. Indian ocean corals reveal crucial role of World War II bias for Twentieth
385 Century warming estimates. *Scientific Reports* 7, 1–11 (2017).

- 386 20. Folland, C., Parker, D. & Kates, F. Worldwide marine temperature fluctuations 1856–1981.
387 Nature 310, 670–673 (1984).
- 388 21. Folland, C. & Parker, D. Correction of instrumental biases in historical sea surface temper-
389 ature data. Quarterly Journal of the Royal Meteorological Society 121, 319–367 (1995).
- 390 22. Freeman, E. et al. ICOADS Release 3.0: a major update to the historical marine climate
391 record. International Journal of Climatology 37, 2211–2232 (2017).
- 392 23. Kent, E. C. et al. Global analysis of night marine air temperature and its uncertainty since
393 1880: The HadNMAT2 data set. Journal of Geophysical Research: Atmospheres 118,
394 1281–1298 (2013).
- 395 24. Kent, E. C. et al. A call for new approaches to quantifying biases in observations of sea
396 sur- face temperature. Bulletin of the American Meteorological Society 98, 1601–1616
397 (2017).
- 398 25. Chan, D. & Huybers, P. Systematic differences in bucket sea surface temperature measure-
399 ments among nations identified using a linear-mixed-effect method. Journal of Climate 32,
400 2569–2589 (2019).
- 401 26. Chan, D., Kent, E. C., Berry, D. I. & Huybers, P. Correcting datasets leads to more homo-
402 geneous early-twentieth-century sea surface warming. Nature 571, 393 (2019).
- 403 27. Carella, G. et al. Estimating sea surface temperature measurement methods using charac-
404 teristic differences in the diurnal cycle. Geophysical Research Letters 45, 363–371 (2018).

405 28. Chan, D. & Huybers, P. Systematic differences in bucket sea surface temperatures caused
406 by misclassification of engine room intake measurements. *Journal of Climate* (2020).

407 29. Laepple, T. & Huybers, P. Global and regional variability in marine surface temperatures.
408 *Geophysical Research Letters* 41, 2528–2534 (2014).

409 30. Karl, T. R. et al. Possible artifacts of data biases in the recent global surface warming
410 hiatus. *Science* 348, 1469–1472 (2015).

411 31. Davis, L. L., Thompson, D. W., Kennedy, J. J. & Kent, E. C. The importance of unresolved
412 biases in twentieth-century sea surface temperature observations. *Bulletin of the American*
413 *Meteorological Society* 100, 621–629 (2019).

414 32. Kent, E. C. et al. Observing requirements for long-term climate records at the ocean
415 surface. *Frontiers in Marine Science* 6, 441 (2019).

416 33. Kennedy, J., Smith, R. & Rayner, N. Using AATSR data to assess the quality of in situ
417 sea-surface temperature observations for climate studies. *Remote Sensing of Environment*
418 116, 79–92 (2012).

419 34. Kennedy, J., Rayner, N., Smith, R., Parker, D. & Saunby, M. Reassessing biases and other
420 uncertainties in sea surface temperature observations measured in situ since 1850: 1.
421 measurement and sampling uncertainties. *Journal of Geophysical Research: Atmospheres*
422 116 (2011).

423 35. Carella, G., Kent, E. C. & Berry, D. I. A probabilistic approach to ship voyage reconstruc-
424 tion in ICOADS. *International Journal of Climatology* 37, 2233–2247 (2017).

425 36. York, D., Evensen, N. M., Martinez, M. L. & De Basabe Delgado, J. Unified equations for
426 the slope, intercept, and standard errors of the best straight line. *American Journal of*
427 *Physics* 72, 367–375 (2004).

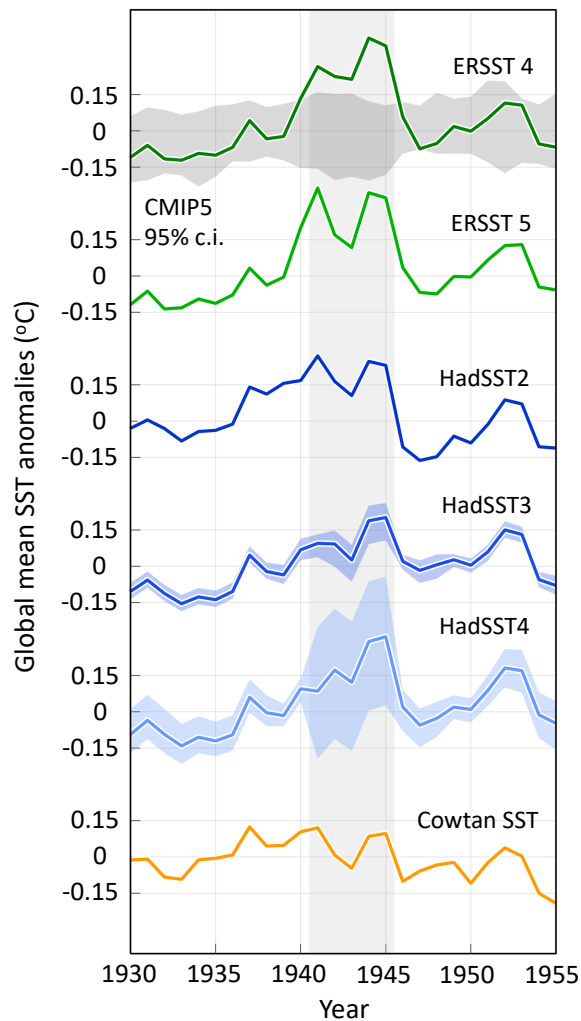
428 37. Woodruff, S. D. et al. Icoads release 2.5: extensions and enhancements to the surface
429 marine meteorological archive. *International journal of climatology* 31, 951–967 (2011).

430

431 **Acknowledgments**

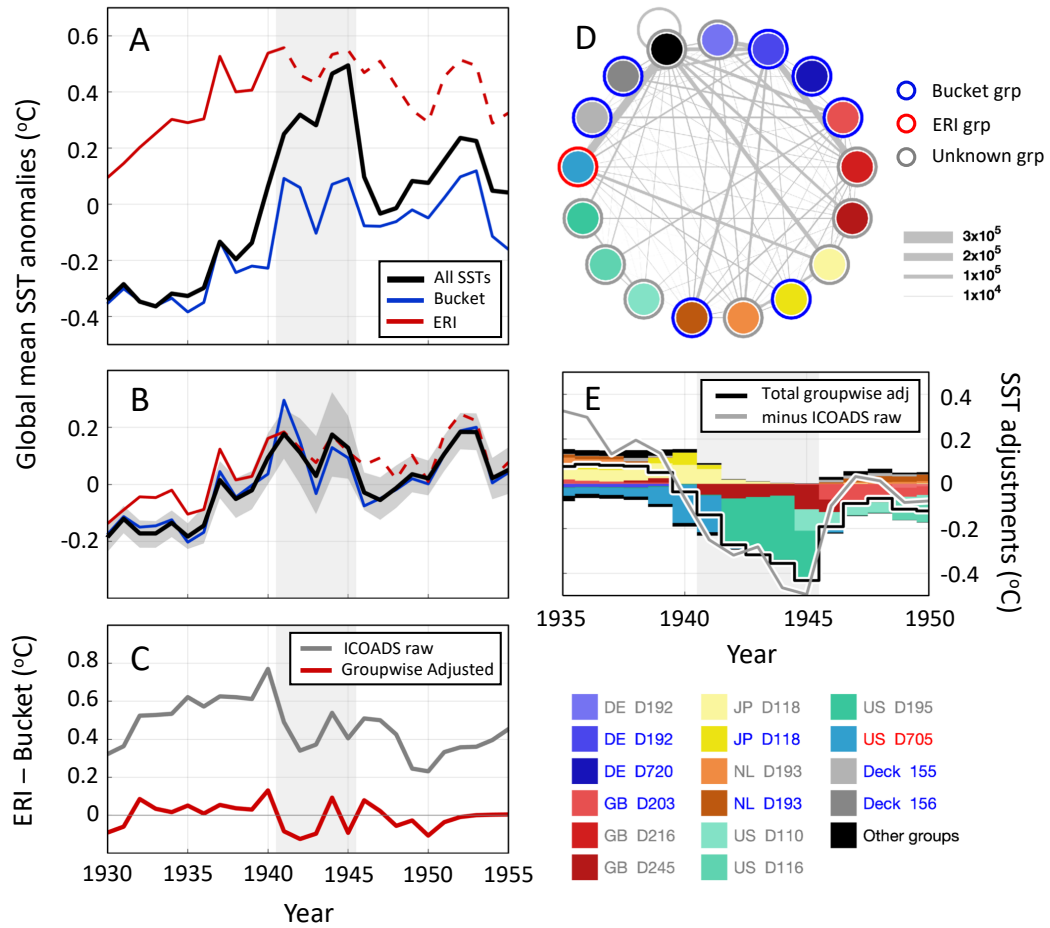
432 **Funding:** This study is funded by a grant from the Harvard Global Institute. **Author**
433 **contributions:** Both authors designed the study, and D.C. led the analysis and writing, with
434 P.H. contributing. **Competing interests:** The authors declare that they have no competing
435 financial interests.

436



438

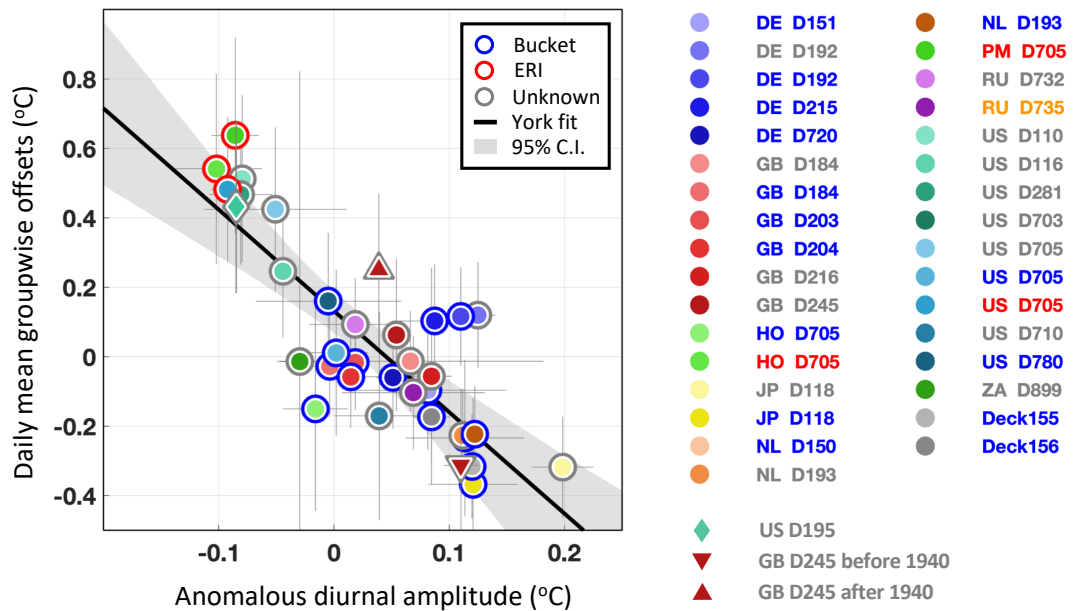
439 **Fig. 1. Various World War 2 Warm Anomalies (WW2WAs).** ERSST4 (dark green), ERSST5
 440 (light green), and HadSST4 (light blue) have SSTs during WW2 that greatly exceed
 441 ($P < 0.01$) CMIP5 historical simulations (gray shading). HadSST3 (medium blue) and
 442 Cowtan SST (orange) do not show an apparent WW2WA. Global-mean SST anomalies
 443 are plotted relative to the average over 1936 to 1940 and 1946 to 1950 and error bars are
 444 95% confidence intervals.



445

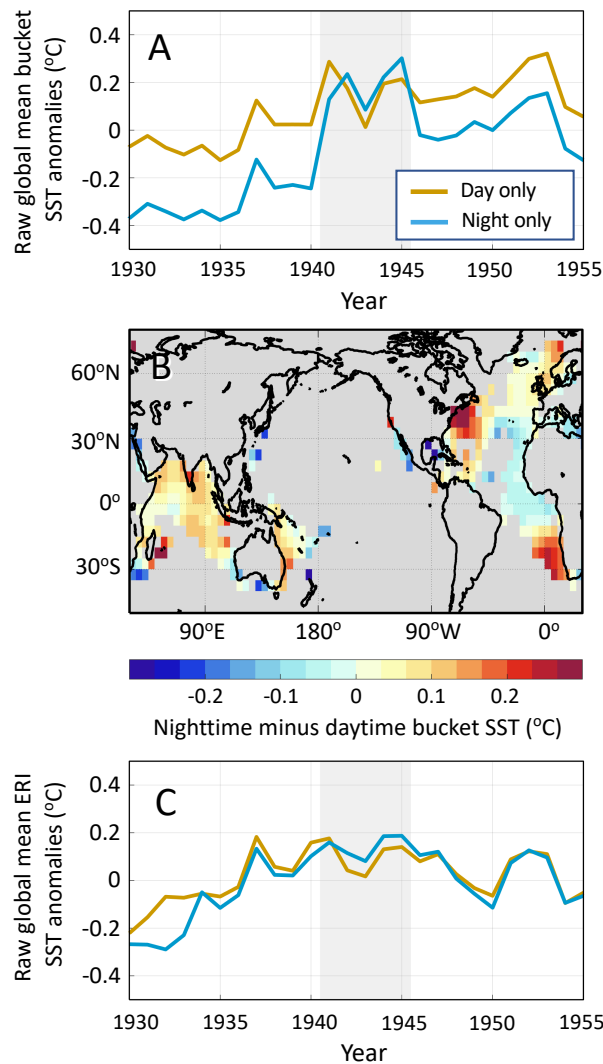
446 **Fig. 2. Linear-mixed-effect method and groupwise SST corrections.** (A), global mean SST
 447 anomalies in raw ICOADS dataset version 3.0. Engine-room-intake SSTs (ERI, red) are
 448 warmer than bucket SSTs (blue) throughout 1930 to 1955. Combining all available
 449 measurements (black) results in a 0.41°C WW2WA that greatly exceeds that in either
 450 bucket- or ERI-only estimates. U.S. measurements without instrumental information
 451 (dashed red) appear consistent with ERI SSTs because they have warm offsets and small-
 452 amplitude diurnal cycles (Fig. 3). (B), as (A) but after accounting for groupwise offsets,
 453 the WW2WA reduces to 0.14°C (95% c.i. 0.02 to 0.27°C , gray shading). (C), the
 454 difference between collocated ERI minus bucket SSTs drops from approximately 0.5°C in

455 raw ICOADS (gray) to being centered on zero after groupwise adjustments (red). **(D)**,
456 numbers of SST pairs (width of connections) between individual groups (filled circles)
457 during 1935 to 1949. Groups are designated according to nation and deck number (inner
458 circle color) as well as instrument type (outer circle color). **(E)**, groupwise decomposition
459 of SST adjustments (stacked bars). Adjustments during WW2 foremost relate to U.S. Navy
460 ship logs (deck 195) and G.B. Royal Navy ship's logs (deck 245). Nation abbreviations
461 are: DE, Germany; GB, Great Britain; JP, Japan; NL, the Netherlands; and US, the United
462 States. Groups having fewer than 100,000 measurements during 1935 to 1949 are labeled
463 as 'other groups'.



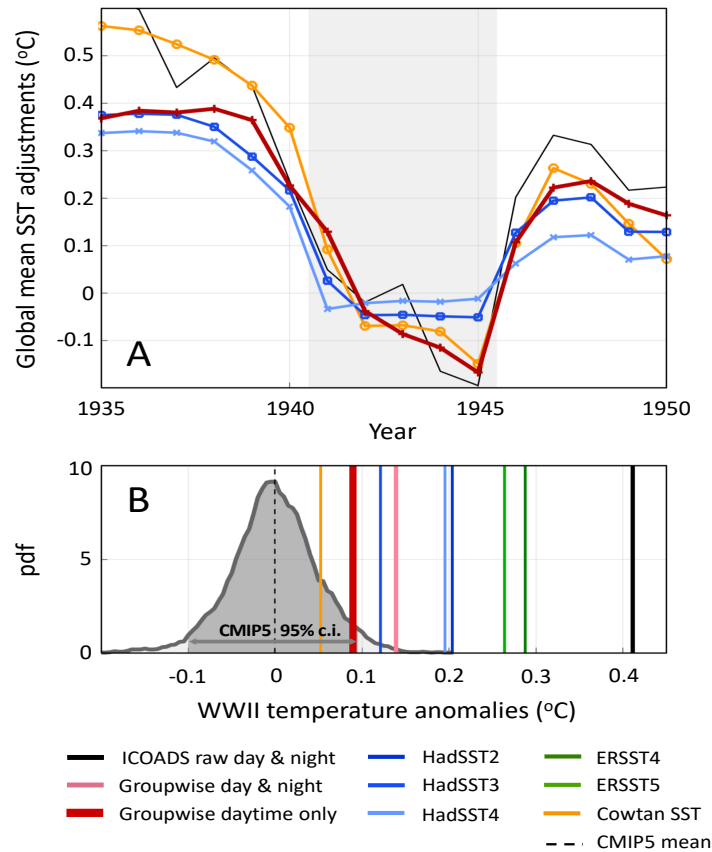
464

465 **Fig. 3. Groupwise offsets scale negatively with amplitudes of diurnal cycles.** Shown offsets (y-
 466 axis) are fixed and five-yearly offsets averaged over 1935 to 1949. Shown amplitudes (x-
 467 axis) are anomalies relative to the 1990 to 2014 climatology from drifters. U.S. deck 195
 468 (diamond) mainly samples at three local hours and has its diurnal amplitude estimated
 469 using a different method (see Fig. S2). Although Great Britain deck 245 always has diurnal
 470 amplitudes significantly ($P < 0.05$) higher than that from drifters, SSTs before the war (1935
 471 to 1939, upward-pointing triangle) are coldly offset by -0.31°C , whereas SSTs after the
 472 beginning of the war (1941 to 1947, downward-pointing triangle) are warmer and have an
 473 offset 0.25°C . Colors of outer cycles denote instruments. 95% c.i.s are estimated from the
 474 linear-mixed-effect model (vertical bars on each marker) and least-squares sinusoidal fits
 475 of amplitudes (horizontal bars). The central estimate of the scaling between diurnal
 476 amplitude and offsets (black line) is from a York regression with the 95% c.i. (gray
 477 shading) estimated by bootstrapping individual groups (28).



479

480 **Fig. 4. Night-time bucket SSTs during WW2.** (A), during WW2, night-time bucket SSTs in raw
 481 ICOADS 3.0 data (light blue) are 0.32°C warmer than in the surrounding ten years and are
 482 0.02°C warmer than daytime bucket SST (orange). (B), spatially, night-time minus
 483 daytime bucket SSTs (shading) are positive over the Indian Ocean and the extra-tropical
 484 Atlantic during WW2 (1942 to 1945). Grid boxes having less than three months of data
 485 are displayed in gray. (C), as (A) but for ERI SSTs, which show no apparent WW2WA.



486

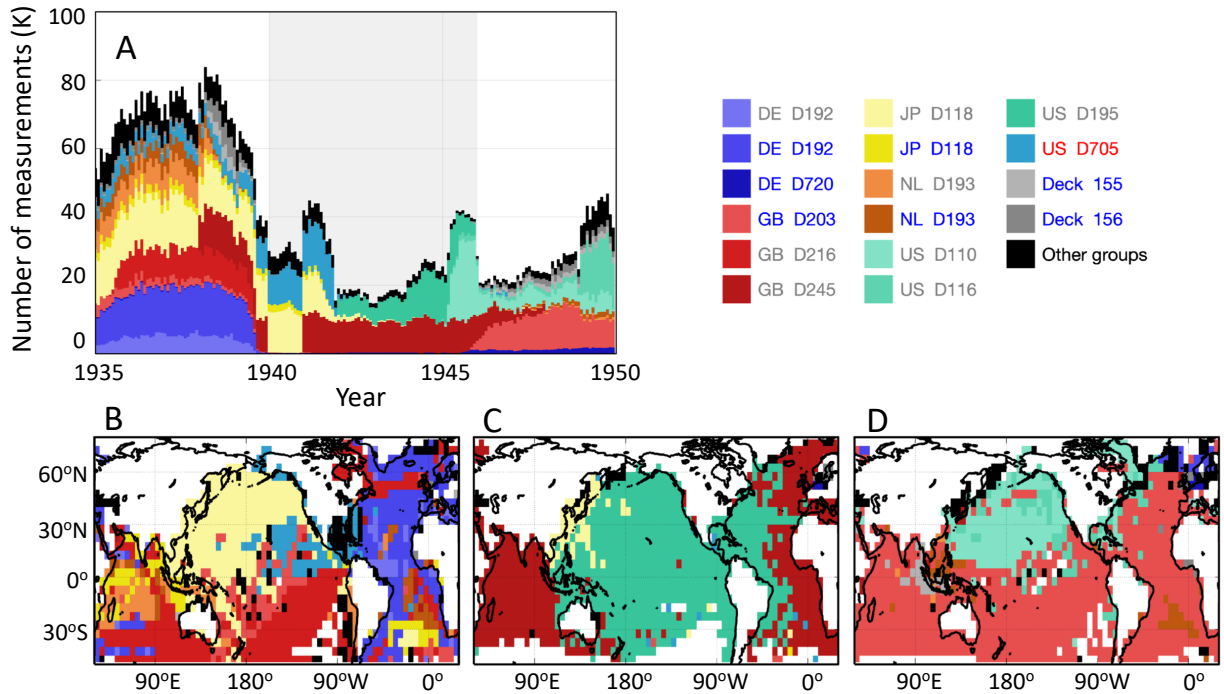
487 **Fig. 5. Comparison against other SST estimates and model simulations.** (A), SST anomalies
 488 from ICOADS 3.0 (black, reversed for purposes of comparison) along with global-mean
 489 SST adjustments from this study (red), HadSST3 (dark blue), HadSST4 (light blue), and
 490 Cowtan SST (orange). Global mean adjustments from this study are calculated as daytime
 491 groupwise- adjusted SSTs minus all unadjusted SSTs and are shifted positively by 0.22°C
 492 for purpose of comparison. (B), WW2WAs (vertical lines) are calculated as the mean
 493 difference between the average over 1941 to 1945 and the average over the ten surrounding
 494 years (1936 to 1940 and 1946 to 1950). Estimates from this study (dark red) and Cowtan
 495 (18) are within the 95% c.i. of internal variability (gray distribution) estimated from CMIP5
 496 pre-industrial control simulations.

497 **Table 1. WW2 SST anomalies and variance.** The WW2WA is defined as the average over 1941-
498 -1945 minus the average over 1936 --1940 and 1946 --1950. Global-mean variance is
499 computed from annual averages from 1936 to 1950, and regional variance is the spatial-
500 average of interannual variance across 5°×5° grids. ERSSTs have lower regional variance
501 because their mapping technique truncates small-scale variability. Cowtan SSTs are only
502 available as global averages. CMIP5 models do not contain sampling and random
503 observational errors and also show lower regional variability. Sampling and random errors
504 cancel under averaging and become negligible at global and decadal scales (26,34). 95%
505 confidence intervals are given in brackets and are estimated from available materials: 1,000
506 random correction members for groupwise-adjusted SSTs, 100 correction members for
507 HadSST3, 200 correction members for HadSST4, 94 simulation members for CMIP5
508 historical runs, and 1,662 15-year segments for CMIP5 pre-industrial control runs.

	WW2 Anomaly (°C)	Global-mean var. (×10 ⁻² °C ²)	Average regional var. (°C ²)
ICOADS (all)	0.41	5.6	0.28
Adjusted (all)	0.14 [0.02, 0.27]	0.8 [0.4, 2.2]	0.22 [0.22, 0.23]
ICOADS (day only)	0.35	4.1	0.26
Adjusted (day only)	0.09 [-0.01, 0.18]	0.5 [0.4, 1.2]	0.21 [0.22, 0.23]
ERSST4	0.29	2.4	0.16
ERSST5	0.26	2.4	0.17
HadSST2	0.20	2.4	0.24
HadSST3	0.12 [0.03, 0.18]	0.7 [0.4, 1.1]	0.21 [0.21, 0.22]
HadSST4	0.20 [-0.09, 0.45]	1.4 [0.5, 5.3]	0.22 [0.21, 0.25]
Cowtan SST	0.05	0.6	--
CMIP5 historical	-0.02 [-0.13, 0.07]	0.5 [0.1, 1.2]	0.13 [0.07, 0.22]
CMIP5 control	0.00 [-0.10, 0.10]	0.4 [0.1, 1.1]	0.13 [0.07, 0.20]

509

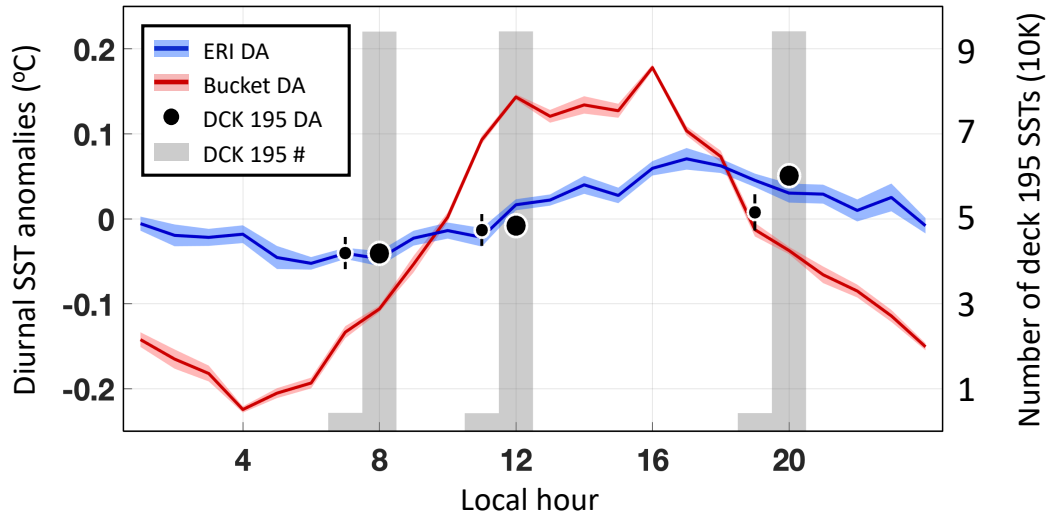
510



512

513 **Fig. S1. Groups of SST measurements.** (A) number of SST measurements from individual
 514 groups identified by country, deck, and instrument. Nation abbreviations are: DE,
 515 Germany; GB, Great Britain; JP, Japan; NL, the Netherlands; and US, the United States.
 516 Groups having fewer than 100,000 measurements between 1935 and 1949 are labeled as
 517 'other groups'. Instruments are indicated by the color of group names for bucket (blue),
 518 ERI (red), and unknown method (gray). (B-D), maps indicating groups that contribute the
 519 most observations within 5° grid boxes for 1936 to 1940 (B), 1941 to 1945 (C), and 1946
 520 to 1950 (D). White grid boxes have fewer than three years of data within corresponding
 521 5-year intervals.

522



523

524 **Fig. S2. The diurnal amplitude of U.S. deck 195.** 96% measurements of SSTs from U.S. deck

525 195 are sampled at 8 am, 12 pm, and 8 pm (gray bars, right y-axis), which does not meet

526 the required minimum number of measurements in each 6-hourly bin in a day for

527 estimating diurnal amplitudes using a sinusoidal fit (27, 28). We, therefore, take an

528 alternative approach that uses diurnal cycles from bucket (red) and ERI (blue)

529 measurements as templates. Diurnal anomalies of bucket and ERI SSTs are obtained from

530 tracked ships over 1935 to 1949 and are shifted such that the mean over 8 am, 12 pm, and

531 8 pm is zero. Unknown U.S. measurements from decks other than 195 are assumed to be

532 ERI measurements. Specifically, diurnal anomalies of deck 195 are represented as a linear

533 combination of bucket and ERI cycles, with the mixture determined using least-squares

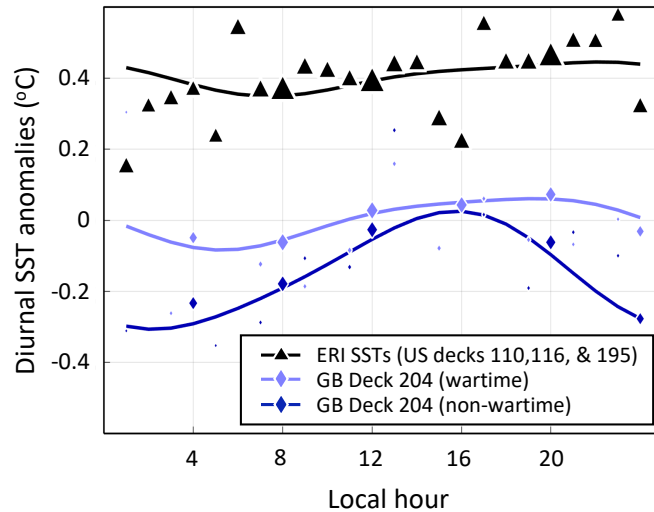
534 fitting. The best fit yields 115% ERI and -15% bucket, equivalent to a diurnal amplitude

535 of 0.04°C that is 0.08°C smaller than that of drifting buoys. A percentage higher than

536 100% should be interpreted as a smaller amplitude than other ERI groups, possibly

537 associated with a deeper sampling depth of large naval ships.

538



539

540 **Fig. S3. Warm biases in night-time bucket SSTs during WW2.** Night-time SSTs from British

541 deck 204 are anomalously warmer during the war (1941 to 1945, light blue) than

542 surrounding years (dark blue). To obtain diurnal anomalies in this figure, we bin all

543 measurements by local hour and calculate the mean in each bin. Such a method is less

544 rigorous than that uses tracked ships (28) but allows for using the maximum amount of

545 data and for a qualitative investigation of offsets between periods. To control noise arising

546 from sampling different regions, we remove collocated groupwise-adjusted daytime SSTs

547 on monthly 5° grids before binning. Results are first calculated for individual years and

548 then averaged over respective periods. Smoothed diurnal cycles are determined with once-

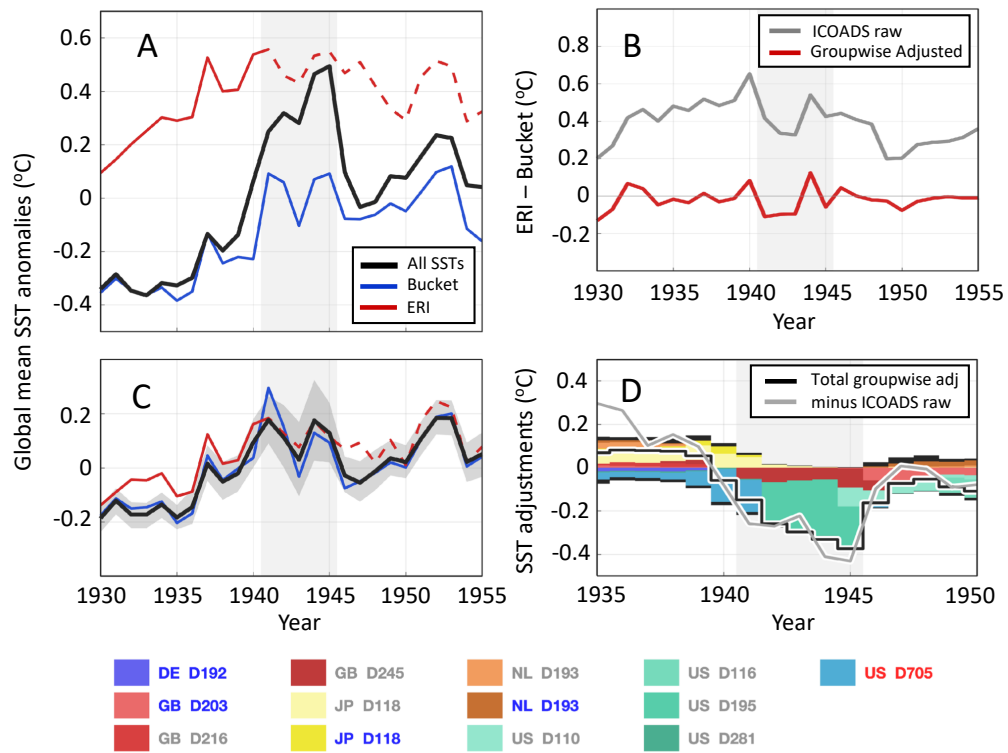
549 and twice-per-day sinusoidal harmonics using a least-square fitting weighted by numbers

550 of measurements in each hourly bin. Also shown are diurnal anomalies of ERI SSTs

551 estimated from U.S. decks 110, 116, and 195. Other U.S. decks are excluded because they

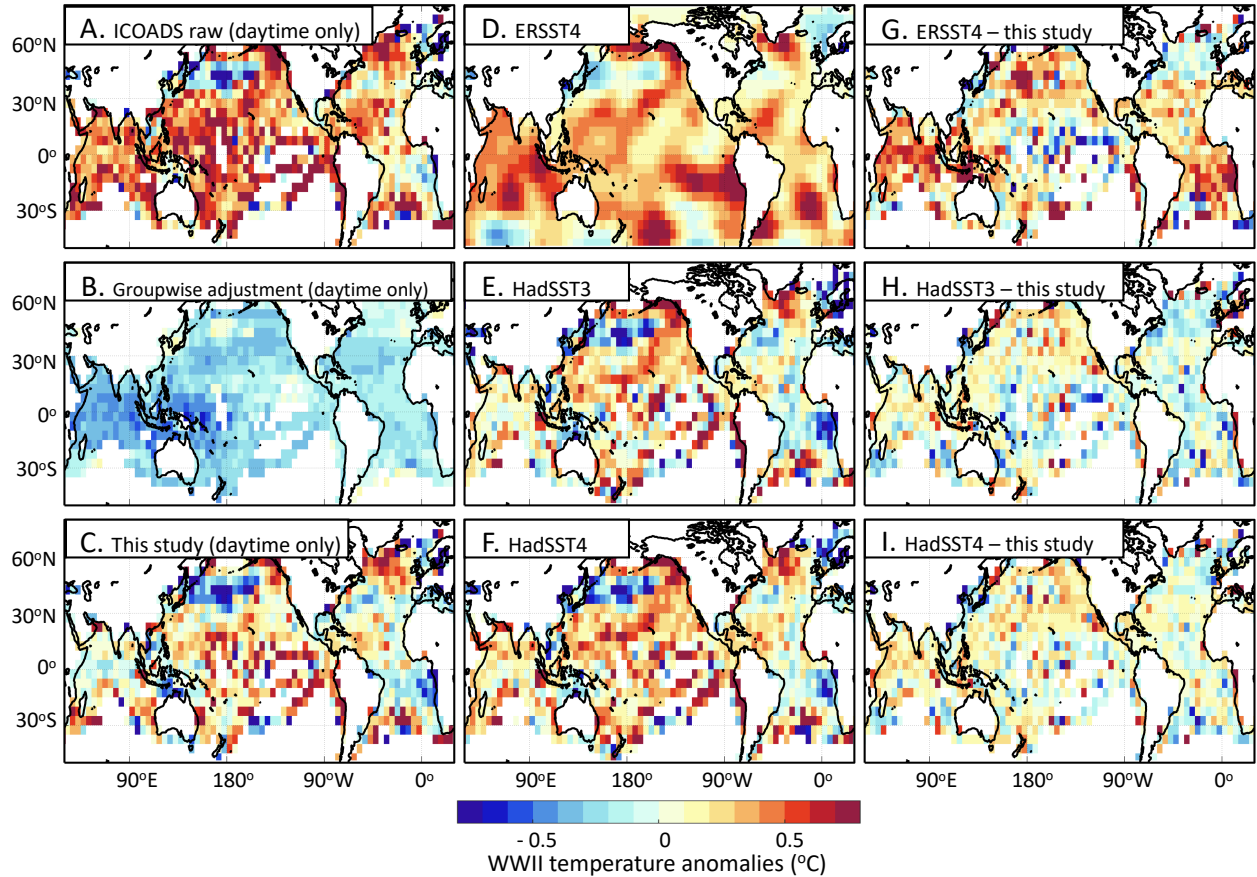
552 take SSTs at fixed Greenwich rather than local hours, which induces additional noise by

553 preferentially sampling certain regions at different local hours.



554

555 **Fig. S4. Groupwise corrections for daytime SSTs.** Individual panels are as those in Fig. 2 but
 556 for the LME analysis that only uses daytime measurements.



557

558 **Fig. S5. Patterns of WW2 SST anomalies.** Shown temperature difference are between 1941 to
 559 1945 and the mean over 1936 to 1940 and 1946 to 1950 for (A), raw daytime SSTs in
 560 ICOADS 3.0, (B), groupwise adjustments of daytime SSTs, (C), adjusted daytime SSTs
 561 (A plus B), (D), ERSST4 (ERSST5 has a similar pattern), (E), HadSST3, and (F),
 562 HadSST4. A grid box is shown if it has at least one year of data that each has at least six
 563 months (a valid year) of observations during 1941 to 1945 and at least one valid year of
 564 data during the ten surrounding years. Also shown are comparisons of our adjusted
 565 WW2WA with other estimates from (G), ERSST4, (H), HadSST3, and (I), HadSST4.

566

567

568 **Table S1. Groups containing SST measurements during 1935 to 1949.** Among 66 groups
569 that have groupwise offset estimates, 33 have valid estimates for the amplitude of diurnal cycles.
570 Shown LME offsets are mean offsets averaged over 1935 to 1949 for the analysis that uses both
571 daytime and night-time SSTs and the analysis that only uses daytime SSTs, respectively. Diurnal
572 amplitudes are anomalies relative to collocated climatology estimated from drifting buoys. ‘*’
573 indicates groupwise offsets differing from zero ($P<0.05$) or diurnal amplitudes differing that of
574 drifting buoys ($P<0.05$). ‘***’ indicates significance after Bonferroni corrections ($P<0.05/66$ for
575 groupwise offsets and $P<0.05/33$ for diurnal amplitudes). Checkmarks highlight U.S. groups with
576 unknown methods, which are assumed to contain ERI SSTs when computing ERI-only estimates.

Group	Nation	Deck	Method ICOADS SI	# of Meas.	Mean offsets	Day offsets	Excess DA	
DE DCK 151	German	Pacific HSST German Receipts	Bucket	3K	-0.10	-0.07	0.08*	
DE DCK 192	German	Deutsche Seewarte Marine	Unknown	259K	0.12	0.13	0.13**	
DE DCK 192	German	Deutsche Seewarte Marine	Bucket	707K	0.12	0.10	0.11**	
DE DCK 215	German	German Marine	Bucket	35K	0.10	0.13	0.09**	
DE DCK 720	German	Deutscher Wetterdienst Marine Met. Archive	Bucket	103K	-0.06	-0.12	0.05**	
GB DCK 184	Great Britain	Great Britain Marine	Unknown	10K	-0.01	-0.02	0.07	
GB DCK 184	Great Britain	Great Britain Marine	Bucket	62K	-0.03	-0.02	-0.00	
GB DCK 203	Great Britain	Selected UK Ships	Bucket	568K	-0.02	0.01	0.02**	
GB DCK 204	Great Britain	British Navy (HM) Ships	Bucket	71K	-0.06	-0.09	0.01	
GB DCK 216	Great Britain	UK Merchant Ship logbooks	Unknown	415K	-0.06	-0.07	0.08**	
GB DCK 245	Great Britain	Royal Navy Ship’s Logs	Unknown	901K	0.06	0.04	0.05**	
HO DCK 705	--	US Merchant Marine Collection (series 500)	Bucket	13K	-0.15	-0.17	-0.02	
HO DCK 705	--	US Merchant Marine Collection (series 500)	ERI	21K	0.54**	0.47**	-0.10**	
JP DCK 118	Japan	Kobe Collection data	Unknown	1056K	-0.32**	-0.28**	0.20**	
JP DCK 118	Japan	Kobe Collection data	Bucket	178K	-0.37*	-0.31*	0.12**	
NL DCK 150	Netherlands	Pacific HSST Netherlands Receipts	Bucket	9K	-0.23*	-0.23	0.11**	
NL DCK 193	Netherlands	Netherlands Marine	Unknown	296K	-0.23*	-0.17*	0.11**	
NL DCK 193	Netherlands	Netherlands Marine	Bucket	227K	-0.22*	-0.20*	0.12**	
PM DCK 705	--	US Merchant Marine Collection (series 500)	ERI	27K	0.64**	0.55**	-0.09**	
RU DCK 732	Russia	Russian Marine Met Data Set	Unknown	52K	0.09	0.02	0.02	
RU DCK 735	Russia	Russian Research Vessel	Hull sensor	1K	-0.10	-0.11	0.07*	
US DCK 110	United States	US Navy Marine	Unknown	402K	0.51**	0.45**	-0.08**	✓
US DCK 116	United States	US Merchant Marine	Unknown	234K	0.25*	0.19*	-0.04**	✓
US DCK 281	United States	US Navy Monthly Aerological Record	Unknown	90K	0.47**	0.41**	-0.08**	✓
US DCK 703	United States	US Lightship Collections	Unknown	17K	-1.08**	-1.02**	0.03	✓
US DCK 705	United States	US Merchant Marine Collection (series 500)	Unknown	26K	0.42**	0.39**	-0.05	✓
US DCK 705	United States	US Merchant Marine Collection (series 500)	Bucket	99K	0.01	-0.03	0.00	✓
US DCK 705	United States	US Merchant Marine Collection (series 500)	ERI	542K	0.48**	0.45**	-0.09**	

US DCK 710	United States	US Arctic Logbooks	Unknown	2K	-0.17	0.02	0.04*	√
US DCK 780	United States	NOAA World Ocean Database	Bucket	9K	0.16	0.11	-0.00	
ZA DCK 899	South Africa	South Africa Whaling	Unknown	13K	-0.01	-0.12	-0.03**	
DCK 155	--	Indian HSST	Bucket	119K	-0.32**	-0.23	0.12**	
DCK 156	--	Atlantic HSST	Bucket	189K	-0.17*	-0.15*	0.08**	
BX DCK 706	--	US Merchant Marine Collection (series 600)	Unknown	5K	-0.10	-0.15	--	
CN DCK 706	China	US Merchant Marine Collection (series 600)	Unknown	1K	-0.38*	-0.43**	--	
DL DCK 706	--	US Merchant Marine Collection (series 600)	Unknown	2K	0.07	0.04	--	
DN DCK 706	--	US Merchant Marine Collection (series 600)	Unknown	3K	-0.12	-0.04	--	
FR DCK 706	France	US Merchant Marine Collection (series 600)	Unknown	7K	0.42**	0.39**	--	
GB DCK 152	Great Britain	Pacific HSST UK Receipts	Bucket	<1K	-0.04	-0.05	--	
GB DCK 202	Great Britain	All Ships (UK MetO MDB)	Bucket	<1K	-0.06	-0.03	--	
GB DCK 205	Great Britain	Scottish Fishery Cruisers	Bucket	4K	-0.43*	-0.39*	--	
GB DCK 705	Great Britain	US Merchant Marine Collection (series 500)	Bucket	18K	-0.12	-0.07	--	
GB DCK 705	Great Britain	US Merchant Marine Collection (series 500)	ERI	11K	0.13	0.08	--	
GB DCK 706	Great Britain	US Merchant Marine Collection (series 600)	Unknown	23K	-0.03	-0.09	--	
GB DCK 707	Great Britain	US Merchant Marine Collection (series 700)	Unknown	<1K	-0.19	-0.26*	--	
HO DCK 706	Great Britain	US Merchant Marine Collection (series 600)	Unknown	<1K	0.05	0.00	--	
HO DCK 707	Great Britain	US Merchant Marine Collection (series 700)	Unknown	<1K	0.09	0.05	--	
IY DCK 706	Great Britain	US Merchant Marine Collection (series 600)	Unknown	6K	0.19	0.20*	--	
JP DCK 705	Japan	US Merchant Marine Collection (series 500)	Unknown	10K	-0.31*	-0.27*	--	
JP DCK 705	Japan	US Merchant Marine Collection (series 500)	Bucket	26K	-0.38*	-0.35*	--	
JP DCK 705	Japan	US Merchant Marine Collection (series 500)	ERI	5K	-0.31*	-0.31*	--	
JP DCK 706	Japan	US Merchant Marine Collection (series 600)	Unknown	8K	-0.26*	-0.28**	--	
NL DCK 705	Netherlands	US Merchant Marine Collection (series 500)	Bucket	10K	-0.21	-0.19	--	
NL DCK 706	Netherlands	US Merchant Marine Collection (series 600)	Unknown	17K	-0.18	-0.14*	--	
NO DCK 706	Norway	US Merchant Marine Collection (series 600)	Unknown	3K	0.34*	0.31**	--	
PM DCK 707	--	US Merchant Marine Collection (series 700)	Unknown	<1K	0.59**	0.46*	--	
RU DCK 735	Russia	Russian Research Vessel	Bucket	<1K	-0.05	--	--	
SP DCK 706	--	US merchant Marine Collection (series 600)	Unknown	<1K	0.01	-0.01	--	
US DCK 116	United States	US Merchant Marine	Bucket	13K	-0.12	-0.14	--	
US DCK 195	United States	US Navy Ships Logs	Unknown	383K	0.43**	0.39**	--	√
US DCK 706	United States	US Merchant Marine Collection (series 600)	Unknown	51K	0.28*	0.29**	--	√
US DCK 707	United States	US Merchant Marine Collection (series 700)	Unknown	2K	0.30*	0.27*	--	√
US DCK 780	United States	NOAA World Ocean Database	Unknown	1K	0.22*	0.20*	--	√
ZA DCK 927	South Africa	International Marine	Unknown	17K	0.01	0.01	--	
DCK 197	--	Danish (and other) Marine (Polar)	Unknown	3K	-0.12	-0.06	--	
DCK 255	--	Undocumented TDF-11 Decks or MDB Series	Bucket	<1K	0.10	0.13	--	

577

578